Observation of the $J/$ and (3686) decays into $^{+}\bar^{-}$

Sun, G. X.; Sun, H.; Sun, H. K.; Sun, J. F.; Sun, L.; Sun, S. S.; Sun, T.; Sun, W. Y.; Sun, Y.; Sun, Y. J.; Sun, Y. Z.; Sun, Z. T.; Tan, Y. X.; Tang, C. J.; Tang, G. Y.; Tang, J.; Tao, L. Y.; Tao, Q. T.; Tat, M.; Teng, J. X.; Thoren, V.; Tian, W. H.; Tian, Y.; Uman, I.; Wang, B.; Wang, B. L.; Wang, Bo; Wang, C. W.; Wang, D. Y.; Wang, F.; Wang, H. J.; Wang, H. P.; Wang, K.; Wang, L. L.; Wang, M.; Wang, Meng; Wang, S.; Wang, S.; Wang, T.; Wang, T. J.; Wang, W.; Wang, W. H.; Wang, W. P.; Wang, X.; Wang, X. F.; Wang, X. L.; Wang, Y.; Wang, Y. D.; Wang, Y. F.; Wang, Y. H.; Wang, Y. Q.; Wang, Yaqian; Wang, Z.; Wang, Z. Y.; Wang, Ziyi; Wei, D.; Wei, D. H.; Weidner, F.; Wen, S. P.; Wenzel, C. W.; White, D. J.; Wiedner, U.; Wilkinson, G.; Wolke, M.; Wollenberg, L.; Wu, J. F.; Wu, L. H.; Wu, L. J.; Wu, X.; Wu, X. H.; Wu, Y.; Wu, Y. J.; Wu, Z.; Xia, L.; Xiang, T.; Xiao, D.; Xiao, G. Y.; Xiao, H.; Xiao, S. Y.; Xiao, Y. L.; Xiao, Z. J.; Xie, C.; Xie, X. H.; Xie, Y.; Xie, Y. G.; Xie, Y. H.; Xie, Z. P.; Xing, T. Y.; Xu, C. F.; Xu, C. J.; Xu, G. F.; Xu, H. Y.; Xu, Q. J.; Xu, X. P.; Xu, Y. C.; Xu, Z. P.; Yan, F.; Yan, L.; Yan, W. B.; Yan, W. C.; Yang, H. J.; Yang, H. L.; Yang, H. X.; Yang, Tao; Yang, Y. F.; Yang, Y. X.; Yang, Yifan; Ye, M.; Ye, M. H.; Yin, J. H.; You, Z. Y.; Yu, B. X.; Yu, C. X.; Yu, G.; Yu, T.; Yu, X. D.; Yuan, C. Z.; Yuan, L.; Yuan, S. C.; Yuan, X. Q.; Yuan, Y.; Yuan, Z. Y.; Yue, C. X.; Zafar, A. A.; Zeng, F. R.; Zeng, X.; Zeng, Y.; Zhai, X. Y.; Zhan, Y. H.; Zhang, A. Q.; Zhang, B. L.; Zhang, B. X.; Zhang, D. H.; Zhang, G. Y.; Zhang, H.; Zhang, H. H.; Zhang, H. H.; Zhang, H. Q.; Zhang, H. Y.; Zhang, J. J.; Zhang, J. L.; Zhang, J. Q.; Zhang, J. W.; Zhang, J. X.; Zhang, J. Y.; Zhang, J. Z.; Zhang, Jiawei; Zhang, L. M.; Zhang, L. Q.; Zhang, Lei; Zhang, P.; Zhang, Q. Y.; Zhang, Shuihan; Zhang, Shulei; Zhang, X. D.; Zhang, X. M.; Zhang, X. Y.; Zhang, X. Y.; Zhang, Y.; Zhang, Y. T.; Zhang, Y. H.; Zhang, Yan; Zhang, Yao; Zhang, Z. H.; Zhang, Z. L.; Zhang, Z. Y.; Zhang, Z. Y.; Zhao, G.; Zhao, J.; Zhao, J. Y.; Zhao, J. Z.; Zhao, Lei; Zhao, Ling; Zhao, M. G.; Zhao, S. J.; Zhao, Y. B.; Zhao, Y. X.; Zhao, Z. G.; Zhemchugov, A.; Zheng, B.; Zheng, J. P.; Zheng, Y. H.; Zhong, B.; Zhong, C.; Zhong, X.; Zhou, H.; Zhou, L. P.; Zhou, X.; Zhou, X. K.; Zhou, X. R.; Zhou, X. Y.; Zhou, Y. Z.; Zhu, J.; Zhu, K.; Zhu, K. J.; Zhu, L. X.; Zhu, S. H.; Zhu, S. Q.; Zhu, W. J.; Zhu, Y. C.; Zhu, Z. A.; Zou, J. H.; Zu, J.. - In: PHYSICAL REVIEW D. - ISSN 2470-0010. - ELETTRONICO. - 106:11(2022), pp. 1-10. [10.1103/PhysRevD.106.112007]

DE GRUYTER

AUTEX Research Journal, Vol. 25, No. 1, 2025, 20250033, DOI 10.1515/aut-2025-0033

DEVELOPMENT OF AUXETIC SHOULDER STRAPS FOR SPORT BACKPACKS WITH IMPROVED THERMAL COMFORT

Eleonora Bianca[1]*, Mariafederica Parisi[2], Daniel Colombo[2], Giuseppe La Fauci[2], Francesca Dotti[1], Ada Ferri[1], Martino Colonna[3]

1 Department of Applied Science and Technology, Polytechnic of Turin, Turin, Italy
2 LSport Technology Lab – DICAM, University of Bologna, Bologna, Italy
3 RE-SPORT srl, Bologna, Italy
*Corresponding author. E-mail: eleonora.bianca@polito.it

Abstract:

Auxetic foams and lattices, characterized by a negative Poisson's ratio, offer unique mechanical and thermal properties that make them promising candidates for next-generation sports and outdoor equipment. This study investigates the application of auxetic materials in the shoulder straps of trekking backpacks to improve both mechanical performance and thermal comfort. First, EVA foam samples were cut using water jet technology to create different auxetic geometries. After conducting tensile tests and digital image correlation analyses, the re-entrant geometry was identified as the most effective. Based on these findings, three types of shoulder straps were developed: a standard model and two auxetic models that differed in cutting pattern (one with undulating and one with linear edges) to evaluate their effects on deformation behavior. After further testing, the auxetic design with wavy edges proved to be superior and was integrated into a fully functional backpack prototype. Tests were then conducted on human subjects to determine whether the auxetic structure improved thermophysiological comfort and load distribution compared to a standard model made from the same materials. The study ultimately led to the development of a patented design for backpacks with auxetic shoulder straps and highlighted their potential to improve the user experience in outdoor applications.

Keywords:

Auxetic materials, materials engineering, thermal comfort, ergonomic comfort, trekking backpacks

1. Introduction

Backpacks are among the most popular load carriers in the world and are used by millions of people in everyday professional or sporting activities [1]. The aspects of comfort, functionality, and safety have a significant impact on performance and safety, as they can affect stability and balance, which can lead to discomfort, pain, and even physical injury, especially in the back and other regions [2].

Regarding spinal health, dimensions, load distribution, and positioning are crucial to the ergonomics of backpacks [1,2]. The scientific literature suggests that the pressure exerted by the weight of the backpack via the shoulder straps could be alleviated by wider straps that better distribute the pressure in this area [3]. Extensive research has investigated the discomfort and muscle fatigue resulting from improper load distribution on the human back [4–7]. Yet, despite numerous studies and comparisons of different backpack models [8,9], manufacturers have insisted on offering largely unchanged designs.

Auxetic materials represent a unique material class that is gaining increasing interest from both academic and commercial perspectives. The word "auxetic" was first used by Evans to describe materials that tend to increase in size due to their negative Poisson's ratio (NPR) [10]. By the Poisson ratio, we refer to the ratio between lateral and axial deformation $-\frac{\epsilon_t}{\epsilon}$ [11]. In line with the classical theory of elasticity, the value of Poisson's ratio for isotropic and homogeneous materials is, in general, between −1 and 0.5 [12].

Usually, conventional materials contract laterally under a tension load, exhibiting a positive Poisson ratio, while, on the contrary, materials with a negative value of this ratio transversely expand when pulled in the longitudinal direction [13]. Various auxetic structures have been discovered in nature and widely reported in the literature; some examples are pyrite [14], cow teat and cat skin, cancellous bone, membranes present in blood cells, and also mother-of-pearl [15].

The first man-made NPR materials ever produced were auxetic open-cell foams in 1987, using a thermocompression process, as reported by Lakes [16]. Foamed materials have many interesting properties, such as their high impact resistance performances, low weight, affordability, extraordinary chemical resistance, and thermal stability, along with the possibility of being recycled [15]. For these reasons, in the past decades, foam materials have gained increasing popularity across the world, being used for everyday life purposes and also representing a promising material to be used in several advanced sports applications [15]. Because of their negative Poisson ratio, auxetic foams can possess enhanced indentation [17,18] and fracture resistance [18] than conventional materials, thus leading to a greater dissipation of energy during an

impact event, as already demonstrated by experimental data [19,20]. Furthermore, the multi-axial expansion [21] and dome-shaped curvature [22,23] of these materials could help improve the overall comfort of protective equipment.

According to the scientific literature, the three typical groups of auxetic cellular structures are re-entrant, chiral, and rotating units [24–29].

Auxetic materials are used in various sports products: both Under Armour and Nike have incorporated auxetic designs into their products [21,30]. The former has developed an auxetic lattice upper that conforms to round or curved shapes for better fit and comfort, while the latter has produced a shoe that incorporates a closed-cell foam outsole with auxetic rotating triangles that can expand bi-axially under certain accelerations and directional changes.

In this work, a new approach to the design of sports backpacks was developed: it aims to introduce new types of shoulder straps with auxetic structures that have a negative Poisson coefficient and are specifically suitable for backpacks. These auxetic shoulder straps can expand when placed under tension by the weight of the backpack and improve ergonomic and thermal comfort due to their hollow structure. First, a series of auxetic patterns were studied to determine the optimal structure and material. These auxetic shapes were materialized on polymer foams using waterjet cutting, and their Poisson ratios were measured by video extensively during a tensile test. Based on the preliminary results, various models of shoulder harnesses were fabricated and tested, and the most promising models underwent a thorough investigation of pressure distribution. Finally, shoulder strap prototypes were made and tested to evaluate their mechanical performance before being integrated into backpack designs.

At the very least, tests have been carried out on humans to assess the effect of auxetic geometry on improving the perception of thermal comfort.

2. Experimental

The experimental procedure is essentially divided into two main approaches: material characterization and human testing. The first led us to select the best combination of structure and geometry for the shoulder straps in terms of mechanical performance, and the second to evaluate the improvement of the auxetic model in terms of thermophysiological comfort.

Rectangular samples of EVA polymer foam, 10 mm thick, 250 mm long, and 60 mm wide, were provided by Fratelli Bertolin Srl (Marostica, Italy). The foam has a density of 100 kg/m^3 and a hardness of 11 Shore A and has already been used for backpack shoulder straps. The material was cut using the water jet punching technique, creating a re-entrant, bi-oriented, and hexagonal pattern. Among these patterns, the re-entrant pattern proved to be the most effective in terms of Poisson's ratio. Based on this result, the first set of shoulder straps (approx. 345 mm × 60 mm × 10 mm) was produced, which has the same external shape as the shoulder straps of the Ferrino Triolet 48 + 5 backpacks.

The straps are made from the same EVA foam but with a different ratio of empty to full volume (the ratio between the void volume and solid volume). For the auxetic straps, the re-entrant cells that had previously been identified as having the largest Poisson ratio were selected. Each cell was 10 mm × 10 mm in size and had a wall thickness of 2 mm.

Thinner walls resulted in mechanical failure when stretched by more than 50% in tensile tests. The cells were arranged vertically within the outer shape of the straps. To prevent mechanical failure, an offset of 2 mm was added along the edges. Previous tests had shown that without this offset, the straps failed in areas where the wall thickness was less than 2 mm. If the addition of the offset reduced the size of the cell by more than 20% of its original dimensions, the cell was removed.

The top and bottom sections of the straps were not perforated to ensure proper attachment to the backpack.

The shoulder strap designs shown in Figure 1 are detailed in Table 1.

Two different geometries of the outer part were chosen (Figure 1), as the elimination of cells below 20% of the shape gave rise to an increased thickness of the outer rim walls. These increased thicknesses affect the Poisson's ratio of the strap since they can hinder lateral expansion. For this reason, wavy (W) and linear (L) straps were produced and tested.

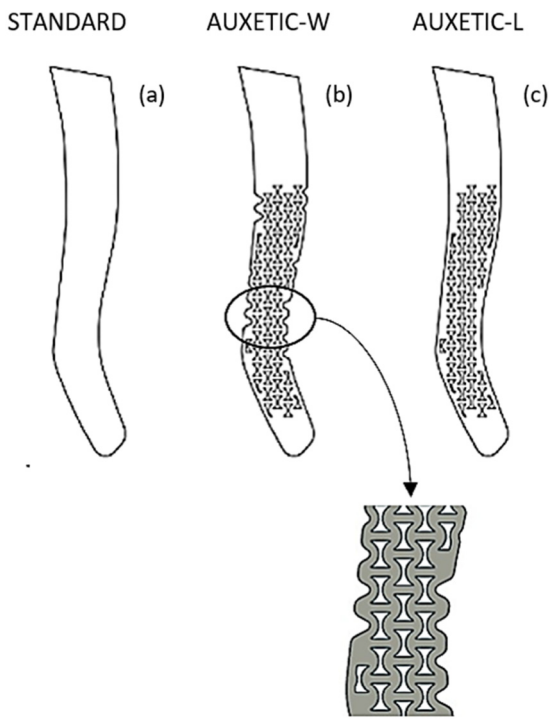

Figure 1. Geometries of the prepared shoulder straps: (a) the standard, non-auxetic structure, and (b) and (c) shoulder straps with an auxetic structure. In (b), the straps feature wavy edges, as highlighted in the magnified view.

Table 1. Characteristics of the shoulder straps produced

Sample	Cell dimension	Offset	Edges	Empty/full ratio
Standard	—	—	Linear	0
Auxetic-W	10 mm × 10 mm	2 mm	Wavy	0.153
Auxetic-L	10 mm × 10 mm	2 mm	Linear	0.149

Furthermore, human tests were conducted to assess the effects of the auxetic structure on human thermal comfort. The subjects participated in activities that resembled real-life scenarios when using the backpack closely. Two different backpack models were studied: a standard model and one with the integration of the selected auxetic geometry into the shoulder straps. Critical parameters such as temperature, humidity, and pressures exerted in the key areas of the backpack were measured to detect significant differences between the samples tested.

2.1. Material characterizations

2.1.1. Tensile test and measurement of Poisson's ratio

Tensile tests and Poisson ratio measurements were performed on samples (consisting of rectangular samples and shoulder straps) using an INSTRON 5966 dynamometer equipped with a 10 kN load cell. These tests were performed at room temperature at a test speed of 50 mm/min. For the central segment of each sample, dot markers were placed at 1 cm intervals to facilitate the calculation of deformations. The tensile tests were recorded using an iPhone 11 camera capturing 4K video at 24 frames/s with an optical zoom of 1×. The distance between the camera lenses and the specimens was approximately 50 cm. The 2D motion analysis functions of the Kinovea software were used to determine both longitudinal and axial displacements so that strains could be calculated from the recorded videos.

2.1.2. Digital image correlation (DIC) measurements

DIC contour plots illustrating the principal strain observed in the tensile tests on shoulder straps were created using GOM Correlate software. The tests were recorded using the Aramis Adjustable M12 system equipped with two cameras (with Schneider 50 mm lenses) recording at a frame rate of 25 frames per second and a resolution of 4,096 × 3,000. These cameras were set up at a distance of approximately 65 cm from the samples and with a stereo angle of 25°. To facilitate the measurements, a pattern was applied to the front of the samples with an airbrush, representing an opaque black spot pattern on a white background. The camera was calibrated using a GOM/CP 40 MV170 card. The images were then analyzed using the GOM Snap and GOM Correlate software.

2.2. Human tests

Ten participants (five men and five women), age 27.9 ± 6.1, were recruited for the *in vivo* tests. All participants were classified as normal weight based on their body mass index (BMI 21.6 ± 2.1). The inclusion criteria for participation were good general health and no musculoskeletal conditions (scoliosis, lordosis, or kyphosis) or injuries that could affect the test results. Participants were informed about the study protocol and gave their written informed consent before participation. This work was carried out according to the principles of the Declaration of Helsinki and under moderate physical and environmental conditions.

2.2.1. Monitored thermal stress parameters

Torso temperature and humidity were collected using Maxim Integrated I-Button DS1923 probes (with a correctable accuracy of ±0.5°C in the temperature range in which they were used) in three body regions: right scapula, left chest, and right deltoid. The mean upper body temperature was calculated according to the guidelines in UNI EN ISO 9886 for the mean skin temperature. The temperature of the torso area was assessed using a modified equation that considers the different weighting coefficients depending on the extension of the area:

$$T_{torso} = 0.417 \times T_{scapula} + 0.417 \times T_{chest} + 0.167 \times T_{deltoid}.$$

As in the temperature calculations, the same equations were used for the mean torso humidity. Furthermore, the temperature and humidity of the skin in the chest area behind the shoulder straps were recorded with MSR 147 probes, providing localized data on the impact of the backpack on this critical area.

Temperature and humidity data were also acquired directly on the outer face of the shoulder straps. This provided insights into the localized effects of the auxetic material on these contact points.

Two variations of the same backpack model were tested: one with auxetic shoulder straps (auxetic-W) and the standard one.

2.2.2. Monitored pressures

The pressure values of the collarbone, pectoral, and armpit were measured before the test in the climatic chamber. The body areas analyzed were identified as the most critical, corresponding to the perforated area of the shoulder straps.

Before starting the measurements, participants were asked to adjust the hip belt, shoulder straps, and chest strap so that the backpack was perceived as comfortable and sat as close as possible to the user's back.

The measurements were carried out using the Picopress pneumatic sensor (Microlab Elettronica, Italy), a flexible, round

plastic bladder with a diameter of 5 cm. Participants were also asked to rate their perception of load and pain at the beginning and end of the tests, and a statistical analysis (Wilcoxon test, $\alpha = 0.05$) was carried out to highlight significant differences between the standard model and the auxetic one. The same protocol was performed only at the end of the test asking the participants to evaluate the perception of friction of the shoulder straps.

To avoid any kind of suggestion, the order of the backpack tested was randomized and kept hidden from the participants.

2.2.3. Experimental protocol

The wear test was conducted in a climate chamber with a controlled temperature of 23.4 ± 0.4°C and a relative humidity of 47.4 ± 0.8%. Participants wore standardized technical T-shirts, shorts, socks, and trainers to ensure uniformity of clothing.

The tests were designed to last a total of 50 min. During this time, participants were required to walk on a treadmill at different speeds and inclinations (10 min at 4 km/h with no inclination, 10 min at 6 km/h at 12% of inclination, 10 min at 4 km/h with no inclination, and the last 10 min at 6 km/h at 15% of inclination). After the 40 min walk, participants were instructed to stand still for a further 10 min.

The tests were carried out on different days at the same time of day to minimize the possible influence of circadian cycles on the participants.

To reinforce to emphasize the effects of the composition of the shoulder straps on participants, the backpacks were loaded with a weight equivalent to 20% of each subject's body weight.

To enhance the understanding of the experimental approach, a flowchart is reported in Figure 2.

3. Results and discussion

3.1. Material characterization

Tensile tests were conducted with both bi-oriented auxetics, re-entrant auxetics, and hexagonal samples to determine the effect of geometry on the mechanical properties and Poisson's ratio.

Based on the tests, it was evident that the standard re-entrant geometry performed better than others in terms of NPR, as shown in Figure 3(a). These values approached −2 within a strain range of 10–20%, indicating superior expansion capability compared to the bi-oriented geometry at low strain. It is noteworthy that certain values of Poisson's ratio ($\nu \leq -1$, $\nu \geq 0.5$) deviate from the assumptions of linear, elastic, isotropic, and homogeneous materials described in the theoretical framework.

Therefore, two auxetic straps were tested to determine the Poisson's ratio and modulus within a strain range of 0–20%. The results of the Poisson's ratio measurements, both in terms of geometry and shoulder strap, are presented in Figure 3 and Tables 2 and 3.

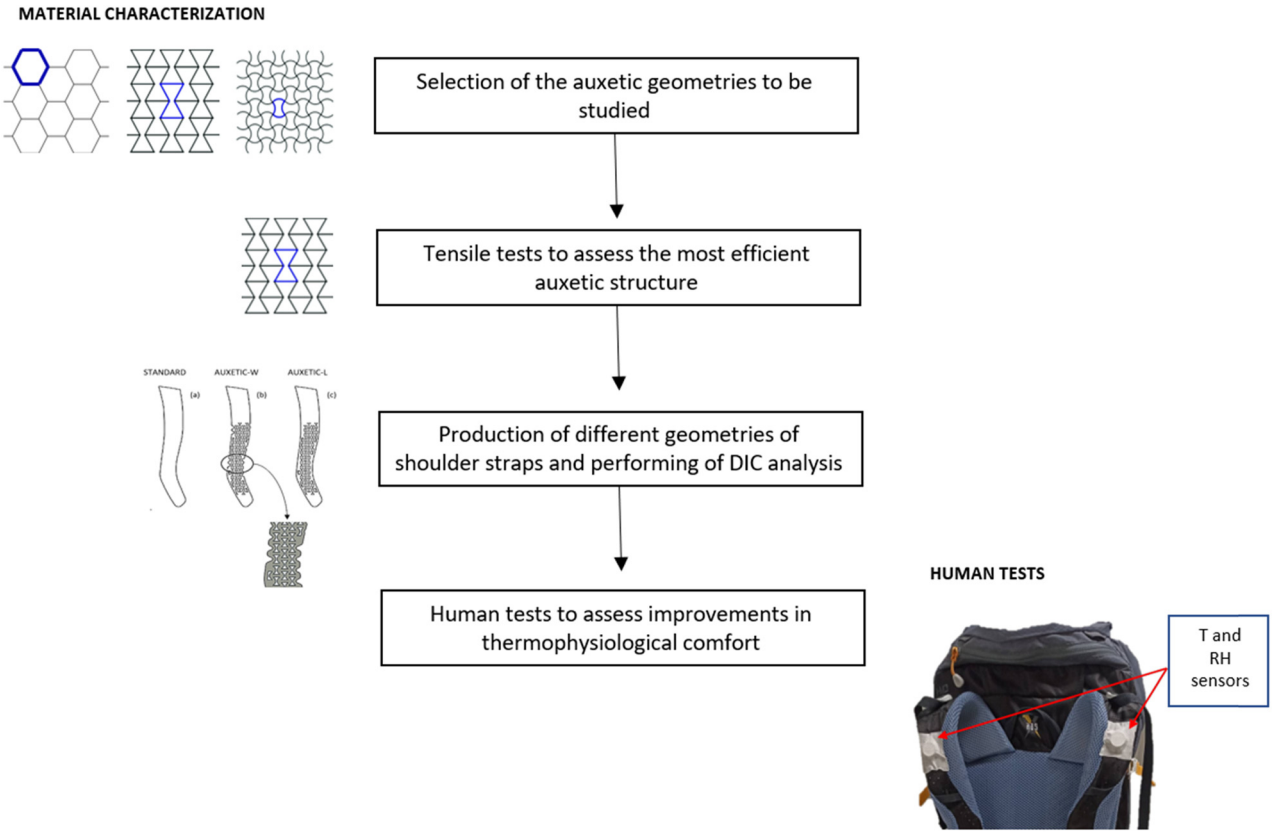

Figure 2. Flowchart of the experimental approach.

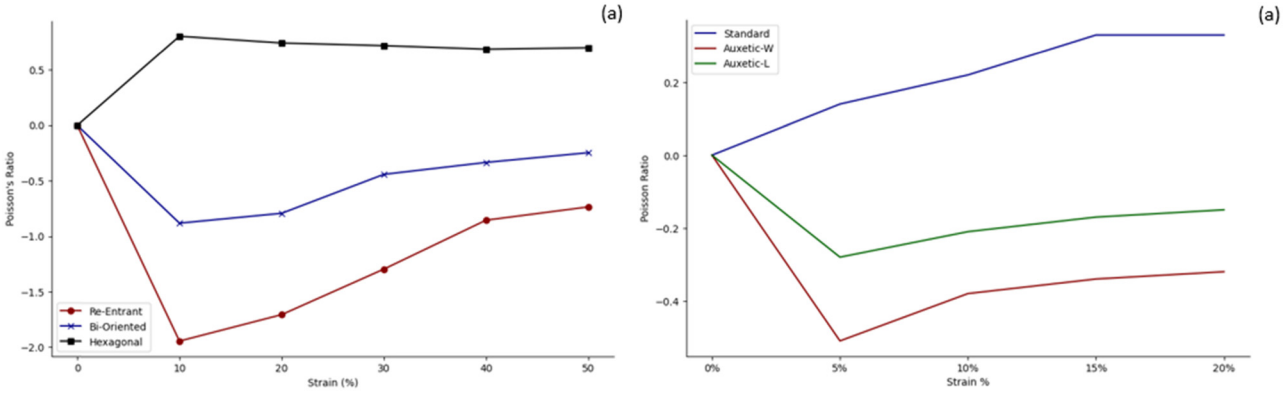

Figure 3. Results of the Poisson's ratio measurements for different geometries (a) and shoulder straps (b).

Consequently, these values should not be interpreted as traditional Poisson ratios within the elasticity theory. Instead, they should be considered as conceptually equivalent measures intended primarily for qualitative assessments.

Hexagonal samples were used as reference specimens, all of which exhibited lower flexibility than the auxetic structures and gave the expected positive Poisson ratio value. Values of the Poisson's ratio for the different geometries compared to the strain (%) are reported in Table 2.

A DIC analysis was performed to observe local deformations that occurred during tensile tests. The DIC analysis of the rectangular samples has shown that an intensification of stresses occurs in the re-entrant geometries due to the presence of sharp corners. The excess stress created in the corners generates breaks at strains above 20%. On the contrary, lower accumulations and no breaks were observed for the bi-oriented re-entrant shape. Therefore, in the design of the geometry to be applied in the following step was rounded in the corners.

Since the elongation of the shoulder straps occurs during use mainly along the longitudinal axis of the strap, a standard re-entrant geometry with the cells oriented along the axis was used for the design of the shoulder strap.

For a more comprehensive view of the properties of the selected shoulder straps, Table 3 resumes the data obtained from the DIC in terms of Poisson's ratio.

The mechanical tests on the shoulder straps showed that a 2 mm wall thickness of the cells was needed to avoid breaks of the shoulder straps below 50% deformation due to stress concentration (as confirmed by DIC analysis). For the same reason, an offset of 2 mm was also applied to the external edges of the strap. In case the external cells have a reduced area of more than 50% concerning the original one, they were eliminated from the design due to the application of the offset. This can generate thicker cell walls on some parts of the edges that can hinder the lateral deformation of the strap. For this reason, a second geometry was developed with a constant cell wall on the edges of 2 mm that was named auxetic-W due to the wavy shape of the lateral edges.

In all the samples examined, the highest value of NPR was reached at about 5% deformation (as reported in Table 3).

The Poisson ratio's measurements (Figure 3) show that the shoulder strap auxetic-W with wavy edges has the highest NPR (of −0.5 at 5% of strain) compared with the auxetic-L due to the lower thickness of the lateral edges, permitting a more efficient expansion of the cells during axial tension.

DIC analysis (Figure 4) also shows that with increasing strain and orientation of the cells, there is a clear tendency for the structure to develop iso-deformation lines in the direction of the applied stress. It is noteworthy that the edges of the auxetic-W exhibited significant local deformation, which is nevertheless far from the yield strain of the material.

This indicates that the shoulder wavy edges sample is capable of providing a significant lateral deformation under load while maintaining its structural integrity and, therefore, has been used to produce a complete backpack for *in vivo* tests.

Table 2. Poisson's ratio of the different structures according to the strain (%)

Strain (%)	Re-entrant	Bi-oriented	Hexagonal
0	0	0	0
10	−1.943	−0.860	0.803
20	−1.705	−0.644	0.724
30	−1.294	−0.233	0.718
40	−0.854	−0.142	0.686
50	−0.734	−0.117	0.796

Table 3. Results at different strains (%) for the three selected shoulder straps from the DIC analysis

Strain (%)	Auxetic-W	Auxetic-L	Standard
0	0	0	0
5	−0.51	−0.32	0.14
10	−0.38	−0.23	0.22
15	−0.34	−0.21	0.33
20	−0.32	−0.23	0.3

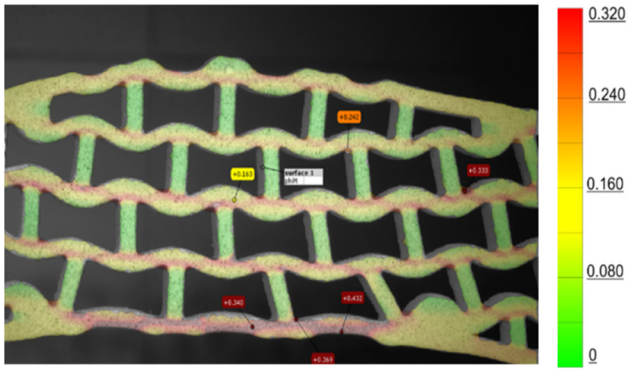

Figure 4. DIC contour plot of the auxetic-W shoulder strap at 20% strain.

3.2. Human tests

3.2.1. Temperature data

Averages were calculated for all data collected by taking the mean across all testers. To provide a measure of the variability or uncertainty around the calculated averages, 95% confidence intervals were calculated.

As shown in Figure 5, a subtle difference was evident. In particular, the torso temperature in the auxetic model had a slightly lower value. This trend persisted throughout the test, in the active phase, except for the last 10 min when participants were standing. This suggests an advantage of the auxetic model in regulating mean torso temperature.

Figure 6 visually shows the temperature distribution in the critical regions for both the auxetic and standard models.

The auxetic model has a lower temperature in the collarbone area, suggesting that it may provide a more comfortable sensation in this region.

Figure 7 contains meaningful data on the temperature variations observed on the shoulder strap. In the case of the shoulder strap, the auxetic model was found to have higher temperature values. This observation, combined with the lower temperatures at the collarbone, suggests that the auxetic material may improve thermal management. It appears to effectively dissipate heat from the subject to the external environment, possibly contributing to improved thermal comfort.

3.2.2. Humidity data

The analysis of mean torso humidity shows that the auxetic model had lower humidity compared to the standard model (Figure 8).

In conjunction with the results on temperature, the analysis of humidity provides additional insight into the performance of the auxetic and standard models. As can be seen in Figure 9, there is a difference in humidity between the two models.

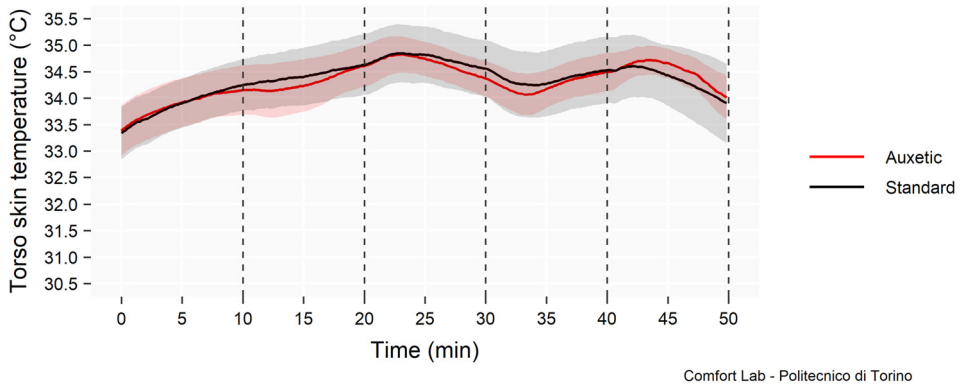

Figure 5. Mean torso temperature with 95% CI.

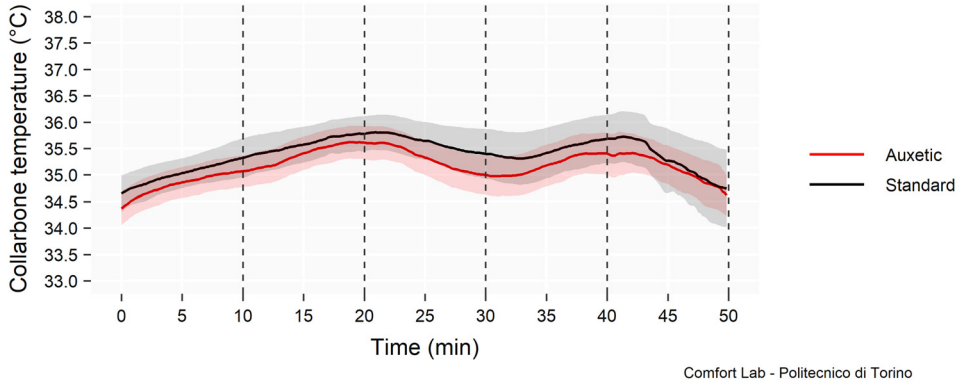

Figure 6. Collarbone temperature with a CI of 98%.

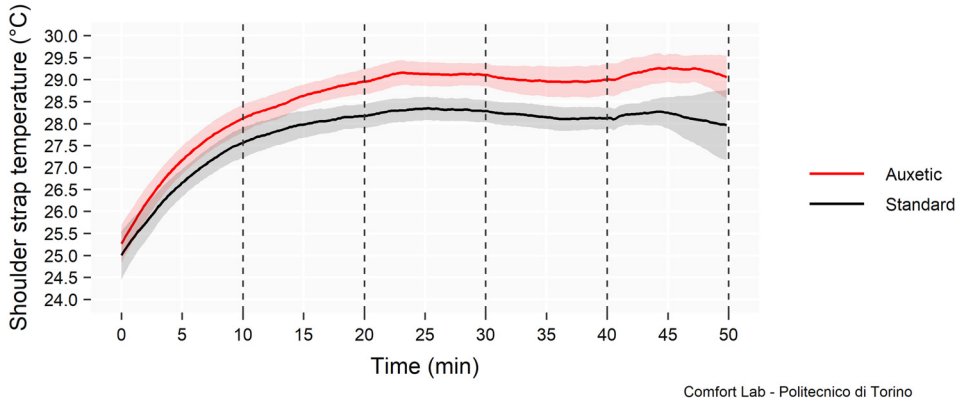

Figure 7. Shoulder strap temperature with a CI of 95%.

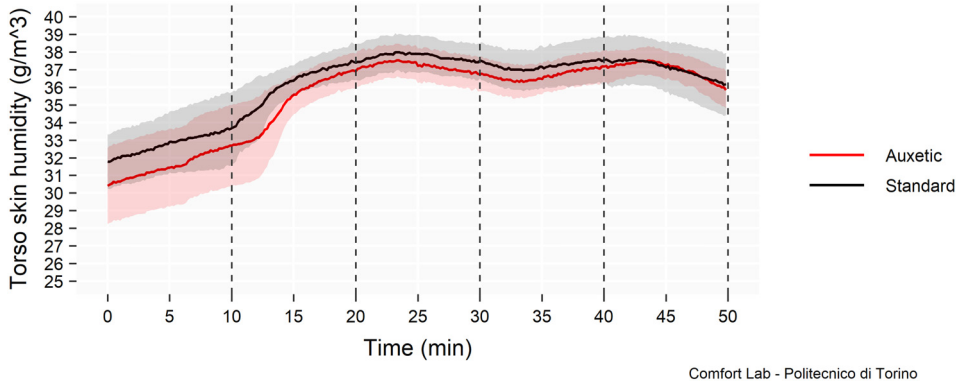

Figure 8. Mean torso humidity with a CI of 95%.

The moisture content of the skin under the shoulder strap was consistently lower in the auxetic model. This fits seamlessly with the earlier observation of improved heat dissipation in this area and shows that the auxetic material offers an advantage not only in temperature management but also in moisture control.

The significant difference in the moisture content of the shoulder straps (Figure 10) indicates again that the material design of the auxetic model plays an important role in moisture management. The auxetic material has consistently lower moisture levels, so it appears to wick sweat and moisture away more effectively at this critical contact point. In addition, the observed difference in the moisture content is consistent with previous results related to temperature. The auxetic model's ability to dissipate heat, reflected in the lower temperatures in key areas, is likely complemented by its superior moisture-wicking properties.

3.2.3. Pressure data

The pressure data measured are shown in Figure 11a with their respective standard deviation.

Even if the statistical analysis shows no statistically significant differences in the pressure exerted by the two backpacks,

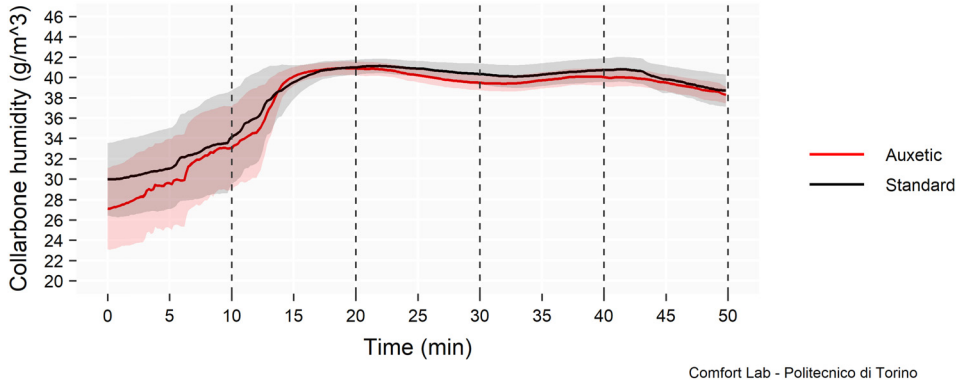

Figure 9. Collarbone humidity with a CI 95%.

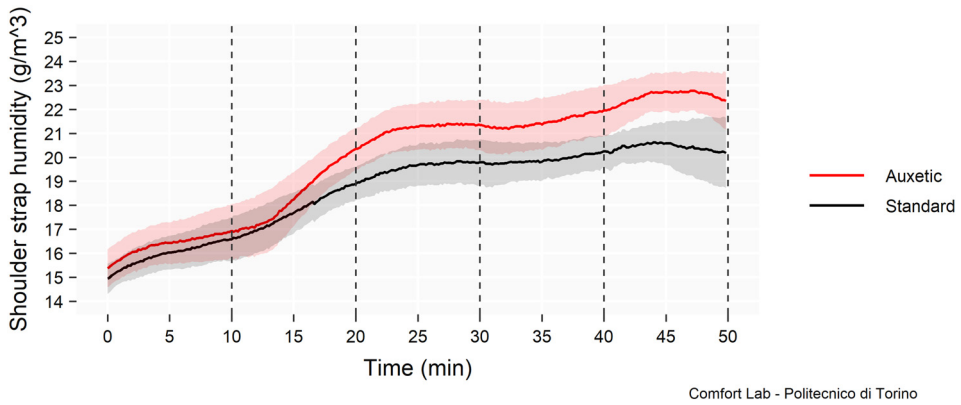

Figure 10. Shoulder strap humidity with a CI of 95%.

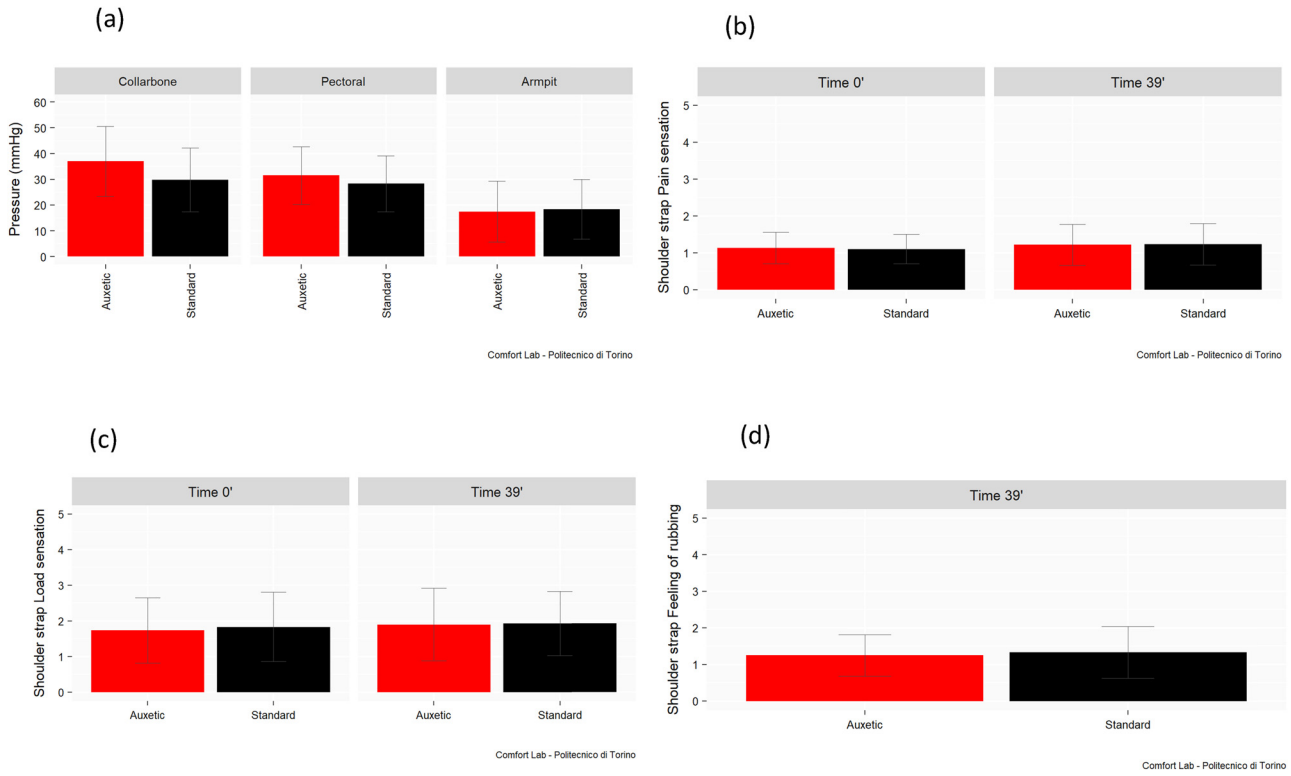

Figure 11. Pressure exerted (a), pressure perceived (b), pain sensation (c), and friction sensation (d).

these results should be evaluated together with the evidence that the surface area in the auxetic model was significantly lower due to the perforation of the auxetic geometry. Given these aspects, it can be said that the auxetic harnesses do not lead to a deterioration in ergonomic comfort.

The subjective assessments of the participants concerning the perception of load carried showed that the Auxetic model provided a slightly better feeling than the Standard one, as shown in Figure 11b.

Regarding the evaluation of pain sensation (Figure 11c), the participants did not find differences. At least, the participants did not report differences in terms of friction sensation at the end of the test, as shown in Figure 11d.

4. Conclusions

The aim of the project was to develop auxetic structures with an NPR that can be integrated into backpacks. A variety of auxetic samples using polymer foams as base material were subjected to initial analysis to determine the optimal design.

Preliminary tests with these patterns showed that the standard re-entrant geometry has the greatest expansion at low loads (5–10%). This characteristic is crucial to ensure optimal comfort and avoid excessive stretching of the shoulder straps. Therefore, for the first batch of shoulder straps, the decision was made to use a re-entrant standard geometry with a material like EVA.

Subsequent testing with this initial group of shoulder straps confirmed that the prototype made with re-entrant structure

and wavy edges had the most favorable auxetic behavior at low strains (with a Poisson's ratio of −0.5 at 5% strain). Further refinements to this shoulder strap design, which included restricting the auxetic geometry to the central section, resulted in improved compression damping compared to fully auxetic geometries. This optimization maintained an NPR at low elongation (−0.32 at 10% elongation).

The in-human tests carried out in the climatic chamber, in which two different backpacks (an auxetic and a standard model) were compared, showed that the auxetic model had significantly better heat and moisture management than the other model tested. The higher temperature and moisture values measured on the outer surface of the shoulder straps, in combination with the lower values on the skin, underline the auxetic geometry's superior ability to dissipate heat and moisture in the most critical areas.

Interestingly, the upper body temperature was lower during the activity phase, indicating efficient heat dissipation. On the contrary, the upper body temperature was slightly higher during the rest phase. These results contribute to higher wearing comfort, especially during physically demanding activities or in warm and humid environments.

The ability of the auxetic material to efficiently regulate moisture on the shoulder straps further enhances its practical benefits. By reducing the accumulation of moisture, the auxetic model offers the user a more comfortable and less clammy feeling, especially when worn for long periods.

At least the auxetic model did not exert higher pressures on the critical areas despite the smaller surface area, which did not impair ergonomic comfort. These data were also confirmed by the participants' subjective assessments of the perception of the load carried, pain, and friction near the shoulder straps.

Acknowledgment: The authors would like to express their sincere gratitude to FERRINO S.p.A. for their valuable and active contribution to the research project.

Author contributions: E.B. – methodology, data processing, and writing, review; M.P. – methodology, data processing, and writing; D.C. – methodology, and data processing; G.F. – methodology and data processing; F.D. – conceptualization of this study, methodology, data processing, and review; A.F. – conceptualization of this study, methodology, review, and funding acquisition; M.C. – conceptualization of this study, methodology, review, and funding acquisition.

Conflict of interest: There is no conflict of interest.

Declaration of interest: The research has been performed in collaboration with the Italian manufacturing company Ferrino s.p.a.

Ethical approval: The conducted research is not related to either human or animal use.

Data availability statement: The datasets generated during and/or analyzed during the current study are available from the corresponding author on reasonable request.

References

[1] *Mallakzadeh, M., Javidi, M., Azimi, S. (2016). Analyzing the potential benefits of using a backpack with non-flexible straps. Work, 54(1), 11–20. doi: 10.3233/WOR-162293.*

[2] *Genitrini, M., Dotti, F., Bianca, E., Ferri, A. (2022). Impact of backpacks on ergonomics: Biomechanical and physiological effects: a narrative review. International Journal of Environmental Research and Public Health, 19(11), 1–19.*

[3] *Abdelraouf, O. R., Hamada, H. A., Selim, A., Shendy, W., Zakaria, H. (2016). Effect of backpack shoulder straps length on cervical posture and upper trapezius pressure pain threshold. Journal of Physical Therapy Science, 28(9), 2437–2440.*

[4] *Liu, B. S. (2007). Backpack load positioning and walking surface slope effects on physiological responses in infantry soldiers. International Journal of Industrial Ergonomics, 37(9–10), 754–760.*

[5] *Lindstrom-Hazel, D. (2009). The backpack problem is evident but the solution is less obvious. Work, 32(3), 329–338.*

[6] *Goh, J. H., Thambyah, A., Bose, K. (1998). Effects of varying backpack loads on peak forces in the lumbosacral spine during walking. Clinical Biomechanics, 13(1), S26–S31.*

[7] *Hong, Y., Li, J. X., Fong, D. T. (2008). Effect of prolonged walking with backpack loads on trunk muscle activity and fatigue in children. Journal of Electromyography and Kinesiology, 18(6), 990–996.*

[8] *Bygrave, S., Legg, S. J., Myers, S., Llewellyn, M. (2004). Effect of backpack fit on lung function. Ergonomics, 47(3), 324–329.*

[9] *Legg, S. J., Barr, A., Hedderley, D. I. (2003). Subjective perceptual methods for comparing backpacks in the field. Ergonomics, 46(9), 935–955.*

[10] *Evans, K. E. (1991). Auxetic polymers: a new range of materials. Endeavour, 15(4), 170–174.*

[11] *Fung, Y. C. (1965). Foundations of solid mechanics, Prentice-Hall, New Jersey.*

[12] *Voigt, W. (1882). Allgemeine Formeln für die Bestimmung der Elasticitätsconstanten von Krystallen durch die Beobachtung der Biegung und Drillung von Prismen. Annalen der Physik, 252(6), 273–321.*

[13] *Mir, M., Ali, M. N., Sami, J., Ansari, U. (2014). Review of mechanics and applications of auxetic structures. Advances in Materials Science and Engineering, 2014(1), 753496.*

[14] *Love, A. E. (1944). A treatise on the* mathematical theory of elasticity*, Courier Corporation, Cambridge.*

[15] *Jiang, Y., Xie, Y., Niu, J. (2024). Short-term dynamic thermal perception and physiological response to step changes between real-life indoor and outdoor environments. Building and Environment, 251, 111223. doi: 10.1016/j.buildenv.2024.111223.*

[16] Lakes, R. (1987). Foam structures with a negative poisson's ratio. Science, 235(4792), 1038–1040.

[17] Doble, M., Kruthiventi, A. K., (2007). Alternate solvents. Green chemistry and engineering, 93–104.

[18] Alderson, K. L., Pickles, A. P., Neale, P. J., Evans, K. E. (1994). Auxetic polyethylene: The effect of a negative poisson's ratio on hardness. Acta Metallurgica et Metalaria, 42(7), 2261–2266.

[19] Lisiecki, J., Błażejewicz, T., Kłysz, S., Gmurczyk, G., Reymer, P., Mikułowski, G. (2013). Tests of polyurethane foams with negative Poisson's ratio. Physica Status Solidi, 250(10), 1988–1995.

[20] Allen, T., Shepherd, J., Hewage, T. A., Senior, T., Foster, L., Alderson, A. (2015). Low-kinetic energy impact response of auxetic and conventional open-cell polyurethane foams. Physica Status Solidi, 252(7), 1631–1639.

[21] Cross, T. M., Hoffer, K. W., Jones, D. P., Kirschner, P. B., Langvin, E., Meschter, J. C. (2013). Auxetic structures and footwear with soles having auxetic structures, Nike Inc.

[22] Wang, F. (2017). Measurements of clothing evaporative resistance using a sweating thermal manikin: an overview. Industrial Health, 55, 473–484.

[23] Sanami, M., Ravirala, N., Alderson, K., Alderson, A. (2014). Auxetic materials for sport applications. Textile Research Journal, 72, 453–458.

[24] Duncan, O., Shepherd, T., Moroney, C., Foster, L., Venkatraman, P. D., Winwood, K., et al. (2018). Review of auxetic materials for sports applications: Expanding options in comfort and protection. Textile Research Journal, 8(6), 241.

[25] Gibson, L. J., Ashby, M. F., Schajer, G. S., Robertson, C. I. (1892). The mechanics of two-dimensional cellular materials. Proceedings of the Royal Society A: Mathematical, Physical and Engineering Sciences, 382(1782), 25–42.

[26] Prall, D., Lakes, R. S. (1997). Properties of a chiral honeycomb with a Poisson's ratio of – 1. International Journal of Mechanical Sciences, 39(3), 305–307, 309–314.

[27] Grima, J. N., Evans, K. E. (2000). Auxetic behavior from rotating squares. Journal of Mechanical Sciences Letters, 19, 1563–1565.

[28] Grima, J. N., Alderson, A., Evans, K. E. (2005). Auxetic behaviour from rotating rigid units. Physica Status Solidi, 242(3), 561–575.

[29] Grima, J. N., Gatt, R., Ravirala, N., Alderson, A., Evans, K. E. (2006). Negative Poisson's ratios in cellular foam materials. Physica Status Solidi, 423(1–2), 214–218.

[30] Sarazyn, J. (2013). Smart Electronic Pet Collar System for training and tracking health, location, and accurate activity levels of pets, US Pat., 13/889,652.